EXS/P2-22

Study of Edge Turbulence from the Open to Closed Magnetic Field Configuration during the Current Ramp-up Phase in QUEST

H. Zushi[1)], N. Nishino[2)], K. Hanada[1)] H. Honma[3)], H.Q. Liu[3)], Y. Higashizono[3)] M. Sakamoto[1)],Y. Nakashima[4)], M. Ishiguro[3)], T. Ryoukai[3)], S. Tashima[3)], K. Nakamura[1)], H. Idei[1)], M. Hasegawa[1)], A. Fujisawa[1)], O. Mitarai[5)], A. Fukuyama[6)], Takeiri[7)], Y. Takase[8)], T. Maekawa[6)], Y. Kishimoto[6)], K. Toi[7)], M. Kikuchi[9)] and the QUEST group

[1)] *RIAM, Kyushu University, Kasuga, Fukuoka, Japan, 816-8580*
[2)] *Mechanical System Engineering, Hiroshima University. Hiroshima, 739-8527, Japan*
[3)] *IGSES, Kyushu University, Kasuga, Fukuoka, Japan, 816-8580,*[4)] *University of Tsukuba*, [5)] *Tokai University*, [6)] *Kyoto University* [7)] *National Institute for Fusion Science* [8)] *The University of Tokyo,* [9)] JAEA

E-mail contact of main: zushi@triam.kyushu-u.ac.jp

Abstract. Statistical features of fluctuations including blobs are investigated using the CCD imaging technique in open and closed magnetic configurations. In a simple open magnetic configuration with vertical (B_z) and toroidal fields (B_t) slab plasma produced by electron cyclotron waves is studied as a function of B_z/ B_t. It is found that fluctuations become dominated by blobs depending on the ratio B_z/ B_t. In the plasma source region R_s helix-sinusoidal perturbations are exited, whose helix angle and vertical wavelength are consistent with pitch angle and turn distance of the magnetic field lines there. Steep gradient in the intermediate region R_{im} outside R_s triggers the plasma to expand radially as a blob ejection. Along the ridge line of the maximum inverse scale length a wave front of the helix perturbation moves outward. Acceleration of a blob is found in the source-free region R_{sf}. It is found that the probability density function pdf of fluctuations in all B_z/ B_t experiments is close to a gamma distribution. Ohmic plasma is ramped-up from the slab plasma and closed surface LCFS is formed. Fluctuations inboard side and outer scrape off layer SOL are studied in this process. Former one is characterized by small amplitude fluctuation level δI/I~ a few %, but latter one shows intermittent large amplitude. Two dimensional structures of the higher moments (skewness S and kurtosis k) representing the shape of pdf are studied. In the former it is observed that these structures consistent with the LCFS, and the pdf is close to a Gaussian distribution. The numerical coefficients characterizing the Pearson system are also derived. In the outboard SOL, it is found that S and k are not only a function of the magnetic flux, but also the magnetic field lines. The pdf is consistent with the Gaussian one for 0.1m from the LCFS, and becomes beta and gamma ones far from the LCFS. Based on the observed numerical coefficients in the Pearson system a relation between pdfs and model of density fluctuation is discussed.

1. Introduction

Turbulence as a coherent structure in the edge region of tokamaks has been considered to play an important role on radial transport in the scrape-off layer SOL and also on maintenance of the high performance of the core plasma [1, 2]. Recently the importance of the role of blob on the convective transport and its effects on the wall loading has been extensively investigated both in experiment and theoretical fields [3-8]. Nonlinear evolution of drift or interchange instabilities driven by the pressure gradient or curvature of the magnetic field lines, the role of the E×B flow in shearing off a radially extended structure, and ejection of a blob are an active area for these subjects. In QUEST blob generation and propagation is studied in slab plasma created by electron cyclotron EC waves with a simple magnetic configuration characterized by open field lines [9]. This situation is similar to that in TORPEX[10]. Identification of initial perturbations, nonlinear evolution of them, trigger mechanisms of a blob by steepening the gradient of the profile, and acceleration of the blob along the excursion has been investigated using two dimensional fast imaging technique [9,11]. During the ohmic start-up phase, a closed magnetic surface LCFS appears from the board side and develops quickly. Helical perturbations along the slab plasma are forced to be

bent due to the closed surface and moved outwards. Since ECWs are continued, there exist two plasma sources input to the SOL plasma from the core ohmic plasma and ECR region vertically localized outside the LCFS. They are possible to drive the SOL fluctuations. The relatively weak fluctuation near the inboard side and intermittent strong fluctuations dominated by blobs in outer SOL are investigated. Blob propagates not only along the field lines and but also radially.

It has been reported that in tokamas, RTPs, stellarators, and linear devices there are fundamental similarities in the radial transport, which is characterized by intermitted convection rather than diffusion, extension into the far SOL, and significant recycling [3-6]. Several types of the probability distribution function pdf *p(x)* are fitted and from the statistic point of view universality of the SOL fluctuations has been proposed. Although the shape of the pdf varies inside, near and far from the last closed flux surface LCFS, it has been pointed out that the pdf belongs to a family of the Pearson type including the Gauss, gamma and beta distributions [12,13]. The pdf is characterized by the mean (μ), variance ($\mu_2=\sigma^2$), mode or anti-mode at which $d(\log(p(x)))/dx=0$, and multimodality. μ denotes the moment and σ is the standard deviation. The higher order moments of pdf represent the shape of pdf, skewness $S=\mu_3/\mu_2^{3/2}$ and kurtosis $k=\mu_4/\mu_2^2$. Instead of k excess kurtosis $k_e=k-3$ is used to focus on the deviation from the Gaussian distribution. These shape factors can be used to understand how the statistics of fluctuations obey the physical stochastic principles. In ref.[12] it has been found that there exists a simple quadratic relation between k and S. Based on this relation plausible pdf in the SOL region is proposed to be beta [13]or gamma distributions[12]. As mentioned early, it is known that theses pdfs satisfy a probability differential equation *PDE*, Pearson system, of form

$$\frac{d(\log(P(x))}{dx} = -\frac{a+x}{c_0+c_1x+c_2x^2} \quad . \tag{1}$$

These coefficients can be derived using these moments [14]

$$c_0 = \frac{(4k_e-3S^2)\sigma}{10k_e-12S^2+12}, c_1 = \frac{S(k_e+6)\sqrt{\sigma}}{10k_e-12S^2+12}, c_2 = \frac{(2k_e-3S^2)}{10k_e-12S^2+12} \quad . \tag{2}$$

We will discuss plausible probability equation for SOL fluctuations. This system includes Gaussian when $c_2=c_1=0$, gamma distribution when $c_2=0$, and beta distribution when the roots for the equation $c_0+c_1x+c_2x^2=0$ are real. The purpose of this paper is to show (1) how widely a simple relation between S and k_e is found in the SOL region, (2) how does this structure obey the change in the magnetic topology, from the open to closed magnetic configurations, and (3) how S and k_e parallel and perpendicular to the field lines behave?

In section 2 experimental conditions and CCD observations are introduced, the results in open and closed magnetic configuration are presented in section 3, statistical analysis is shown in section 4. A relation between pdf and simple models for density fluctuation will be discussed and finally concluding remarks are given.

2. Experimental setup and fast camera imaging

QUEST is a medium sized spherical tokamak, whose major and minor radii are 0.68 and 0.4 m, respectively. There are two flat divertor plates at b (± 1 m) from the mid-plane. Fluctuation measurements have been studied in two different plasma configurations. One is slab plasma which is characterized by an open configuration with both toroidal B_t (~ 87.5 mT) and vertical B_z (< 40 mT) field components without plasma current (I_p < 1 kA). The other is

ohmic plasma including current ramp-up plasma of ~ 50 kA. Fluctuations are studied in a wide SOL. Hydrogen plasma is initiated by microwaves at 2.45 GHz (or 8.2 GHz for the latter) using electron cyclotron resonance heating ECRH. It extends vertically near the resonance layer R_{res}(~ 0.30 m) corresponding to the resonant field, and diffuses outward depending on Rf power and B_z/B_t. Three radial regions are defined; the "plasma source" region, $|R_s|$= 0.45 ~ 0.6 m, which is bounded by a relatively sharp boundary, and "intermediate" (0.6 < $|R_{im}|$ < 0.8 m) and "source-free" ($|R_{sf}|$ > 0.8 m) regions. R_{im} is characterized by a steep light gradient region near the plasma boundary and R_{sf} is by very weak intensity region or essentially vacuum. On the other hand, for ohmic case a plasma source region corresponds to the last closed flux surface LCFS and a source-free region is at least 0.2 m far from the LCFS in the

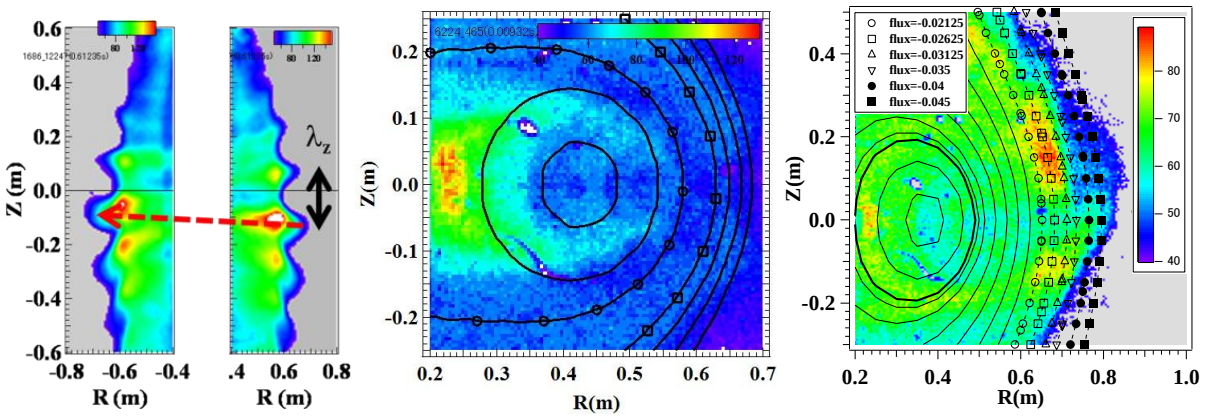

Fig.1 Sinusoidal perturbation in slab configuration (a), ohmic start-up (b), and wide SOL in ohmic plasma. Solid curves are calculated (b) and reconstructed (c) magnetic surfaces. Dashed arrow in (a) indicates alignment of the perturbation along the magnetic field lines.

outer SOL. An intermediate region is considered 0-0.2 m from the LCFS. Since ECWs are continued, the plasma source along the vertical zone at R=R_{res} outside the LCFS must be taken into account.

The K-5 (SA5) fast cameras was used for these experiments. Each frame is made up of 288×240 (526×240)pixels, and framing rate is 20000(50000) frames s^{-1}. Comparison with images using an H_α filter indicates that the observed visible image is mainly attributed to the H_α emission ($\propto n_0 n_e$). In order to analyze temporal and spatial evolution of images it is assumed that the neutrals n_0 are distributed uniform in the chamber and images are due to the local evolution of plasma or propagating plasmoid whose electrons n_e can excite neutral atoms immediately [2-3]. Three images are shown in Fig. 1, which correspond to the slab plasma with a helix-sinusoidal perturbation, ohmic start-up plasma with an

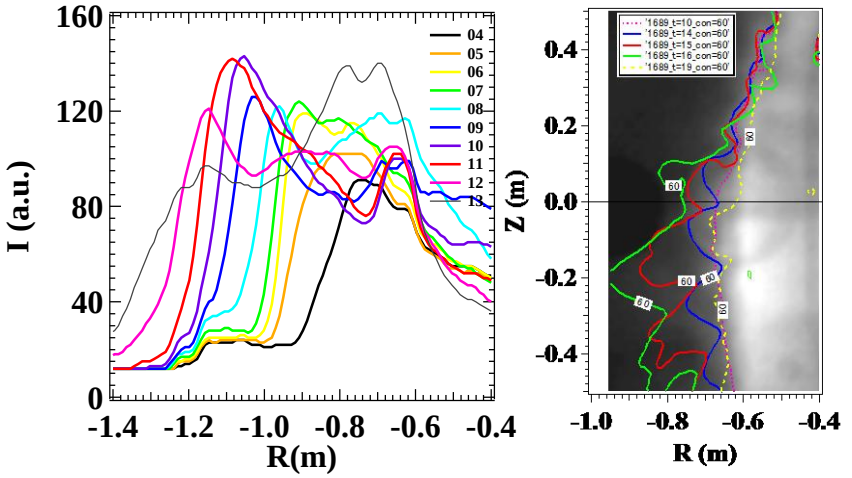

Fig.2(a) Temporal evolution of I(R,t). Time interval is 50 μs.
(b) Iso-intensity curves during the non-linear process are plotted for two cases of B_z/B_t (left=4% and right=20%). The intensity level (I=60 a.u.) is almost the half of the maximum near the source-region

inboard fluctuation zone and established ohmic plasma with a wide outer SOL.

3. Experimental results

3.1.1 helix-instability and blob generation in a slab configuration

It has been observed that fluctuations in this configuration depend on the ratio B_z/B_t. Two kinds of aspect of fluctuations are investigated; helix-sinusoidal perturbation which locates around R_s and blobs which propagate from R_{im} towards to R_{sf} dynamically. First, various properties of helix-sinusoidal perturbations are investigated with respect to those of the magnetic field lines. When the ratio B_z/B_t is varied, the return distance Δ_z ($=2\pi RB_z/B_t$), pitch angle $\theta(=\tan^{-1}(B_z/B_t))$ and the length $L_c(=2\pi R2b/\Delta_z)$ connected to the flat plates of a field line in the poloidal plane are changed. Under present conditions, these parameters at R~ 0.7 m (near the second harmonic position) are changed as follows;$\Delta_z \leq 1.2$ m, $-4° \leq \theta \leq 15°$, and 7.6 m $\leq L_c \leq \infty$. Helix angle and vertical wavelength λ_z of initial helix-sinusoidal perturbations can be determined from the image. Here λ_z is denoted in Fig. 1(a). Fairly good agreement of observations with Δ_z and θ indicates that initial perturbations are excited at R_s and extended along the magnetic field lines there[9]. The relative fluctuation level $\delta I/I$ at R_s is ~ 5% at $B_z=0$ and increased ~ 25 % with increasing B_z. Although the line tying stabilization effect would be expected by increasing B_z and decreasing L_c, the amplitude of fluctuations and their nonlinear evolution become large and significant with increasing B_z/B_t. The evolution of I(R,t) is shown in Fig. 2(a). It is observed that a blob is formed when the plasma boundary is expanded by steeping the gradient at R_{im}, which is caused by the radial growth of these sinusoidal perturbations. The wave-front with the steep gradient moves outwards, however, since the folding point of the gradient moves relatively slow, the gradient becomes more steep. When the folding point reaches at R_{sf}, the speed of the radial expansion is enhanced, i.e., the blob seems to be accelerated. Thus the intermittency of the light intensity becomes significant with increasing R, that is, $\delta I/I$ increases ~ 100 % at R_{sf}. It is observed that Z profiles at R_s change insignificantly, and sinusoidal perturbations remain even during the blob ejection process. This suggests that plasma production rate is not affected by the blob ejection. Temporal evolution of the images including the blob ejection is also studied in the R-Z plane as a function of B_z/B_t. Two-dimensional image at the initial time of a certain cycle, whose peak intensity is 100-120 (a.u.) at R_s, is shown in Fig. 2(b). Evolution of contours of I=60 (a.u.) becomes complex with increasing B_z/B_t from 5 % to 20 % (not shown). For 5 % case the amplitude of perturbations grows in time but a basic sinusoidal structure is relatively kept for 0.45 ms (one cycle). On the other hand, the 20 % case it is shown that perturbations grow nonlinearly in time of 0.65 ms and space from R_s to R_{sf}, and finally a blob is formed from the distorted portion. The radial excursion, non-linear growth of the initial perturbation, is studied by tracing the contour of a given value. The radial excursion for B_z/B_t=5 % is evaluated 0.2-0.3 m as the distance of a wave crest from source intensity structure. On the other hand, for B_z/B_t=20 % case, the radial excursion is quite large (> 0.4 m) and its evolution cannot be viewed as simple growth of sinusoidal perturbation. The effect of B_z/B_t on helix-sinusoidal perturbations is left for future.

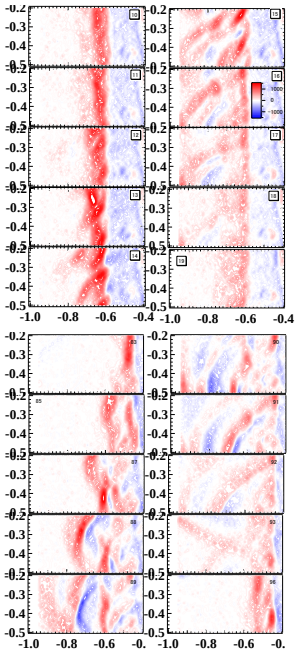

Fig.3 Snap shot of L_p^{-1} in the R-Z plane for 0.5ms. (top) B_z/B_t=5% and (bottom) B_z/B_t=20%. *Figures are displayed in sequential order. Deep red indicates negative* $\nabla_R I$ *and blue positive one.*

3.1.2. Non-linear process of Blob propagation and acceleration

According to Fig. 2 it is suggested that radial gradient or inverse

scale length L_p^{-1} (=$I/\nabla_R I$) outside the source region plays an essential role for a blob to propagate outward. Here ∇_R means radial derivative at a fixed Z position. Thus evolution of $L_p^{-1}(R)$ is studied as a function of B_z/B_t. For B_z/B_t =5 % $|L_p^{-1}(R, t)|$ is small for -0.6 < R_s < -0.5 m and does not change in time. The peak location of $|L_p^{-1}(R, t)|$ starts to expand and to move outwards by 0.2 m within 0.2 ms, that is, with velocity of ~ 1 km/s. When the blob reaches to R_{sf}=-0.8 m, however, blob seems to be accelerated, which is suggested by bending of the ridge. For the case of B_z/B_t=20 % similar ridges are found. The initial propagation velocity of the blob is ~ 0.5 km/s in the intermediate region, but the velocity is increased to ~ 1 km/s towards wall. Thus although the initial propagation velocity from R_s depends on the ratio of B_z/B_t, it should be noted that acceleration of the blob is seen along the path. Figure 3 shows the snapshot at every 50 μs of the contour of L_p^{-1} in the R-Z plane (-1 <R< -0.4 m, -0.5 <Z<-0.2 m) for a certain cycle of blob ejection. The steep gradient (deep red) outside the plasma source region (blue) is deformed and a ridge crest propagates as a blob along and crossing the magnetic field lines. It is noted that the ridge crest propagates along a R-Z trajectory, and does not move simply radially. For B_z/B_t=20 % (Fig. 3 b) the pattern of the contour of L_p^{-1} becomes more complicated. Behind the front of the ridge there is a negative gradient region indicating the clear separation of the main source region and a long tail of the blob.

3.2. Inboard and outboard fluctuation in ohmic plasma

Ohmic plasma is evolved from the inboard side near the ECR slab plasma when the inductive field (< 5V/m) is induced. As Ip is ramped-up and the LCFS grows, the slab plasma is bent outwards significantly. Fluctuations appear inboard side, extend vertically and slightly bend along the LCFS. The intensity of the fluctuations grows as I_p grows and saturates for a few msec. The vertical extended zone is due to the field lines winding round the center stack CS. The connection length just outside the LCFS becomes short because the field lines intersect the center stack, however, outside it the length is unperturbed. This has been confirmed by Li beam measurement during the rf induced current jump phase in the CPD device [15,16]. Thus, two inboard and outer fluctuations are separated each other. In Fig. 1(b) it can be seen that the intensity around the magnetic surface denoted by circles is lower than those of inner and outer (squares) regions. The fluctuation level δI/I is ~ a few % for inboard fluctuation. The ratio of μ and σ is shown in Fig. 4(a). Data are taken for 2 ms at I_p~ 10 kA. Although the highest μ is localized near the CS on the mid-plane, the boundary of the ratio, denoted by black solid curve, follows the LCFS. Outside this boundary the statistics feature is different, as will be mentioned in section 4. At I_p ~ 50 kA the outboard fluctuation in the outer SOL shows again strong perturbations, compared with the quiet inboard fluctuation. Since 70 kW ECWs are continued to be injected and interact to the SOL plasma at the top and bottom region outside the LCFS along the vertical line at R=R_{res}, the plasma source due to ECWs is considered to be dominate this

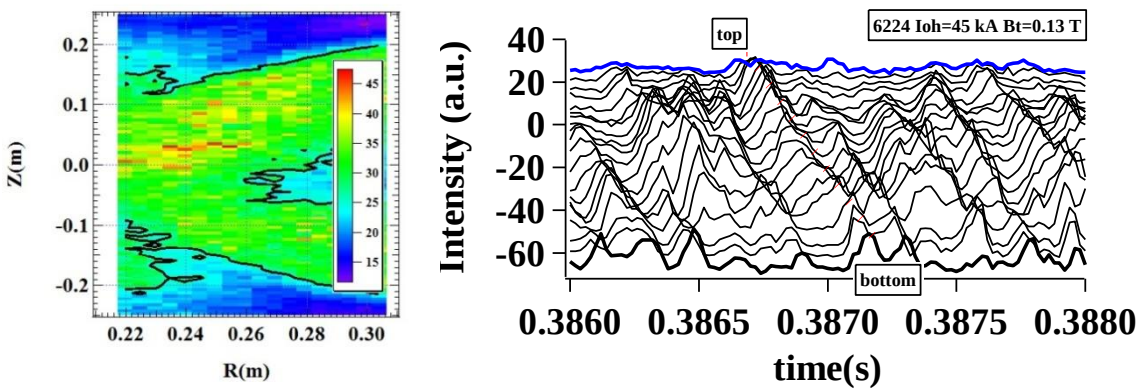

Fig4. (Left) The image of the ratio μ/σ of the inboard fluctuation during the ohmic ramp-up phase. The black contour corresponds to the level 26. Note the vertical and horizontal scales are different. (right) Temporal evolution of I(R,Z,t) along the magnetic field lines from the top to bottom regions. The intensity is plotted with an offset in the vertical coordinate.

SOL region. The temporal evolution of I(R,z,t) is shown in Fig. 4 (b). The intermittent plasma intensity evolution is observed and the blob propagates clearly from the top to bottom and also radially. This direction is the ion drift direction. The frequency of the blob is ~ 2 kHz.

4. Statistics of the CCD light fluctuations in slab and ohmic plasmas

It has been reported that the density and potential fluctuations in the SOL show typical non-Gaussian statistics, that is, the Skewness S is negative or zero in the core, positive in the SOL and tends to increase with the distance from the LCFS [12,13]. In the present research the statistics of two kinds of fluctuations of CCD light are investigated with respect to the magnetic configuration. First, in the slab plasma fluctuations with the large coherent structure controlled by B_z/B_t in the wide spatial area (0.6 m ×1 m) without a certain boundary of the magnetic topology, i.e. LCFS, are surveyed. For B_z/B_t =5 % S is ~ 0.5 at R~R_s and is increased ~ 4 at R~R_{sf}. For B_z=0 S(R_{sf}) is remained less than 0.5, but for $B_z \neq 0$ the intermittency of the fluctuations is usually observed in the R_{sf} region. In B_z/B_t scan experiments it is analyzed that data taken from R_{sf} to the R_{sf} obey a relation k_e~ (1.3-1.5)S^2, as shown in Fig.5. Data points cover typical three radial regions in all B_z/B_t experiments. Observations are similar to those in refs. [12,13]. Secondly, a relatively narrow region(0.5 m ×0.09 m) is studied during ohmic start-up phase of I_p~ 10 kA. Two dimensional contours of S and k_e are shown in Fig.6 (a,b). S ranges from -1 to 1 except the upper left region and it is small positive within LCFS. k_e also ranges within ± 2 and almost zero on the mid plane. These suggest that the pdf is close to the Gaussian distribution. The *PDE* mentioned in Introduction is examined substituting observed quantities into eq. (2). The coefficients c_0, c_1 and c_2 of denominator are derived and shown in Fig. 6(c-e). c_0 is large positive (> 5) in this area and relatively smaller values 2-3 follows the LCFS. c_1 shows a clear boundary corresponding to the LCFS. Outside it c_1 is <-1, and inside the closed flux -1<c_1<1. c_2 is zero in whole region except upper region. These 2D structures of numerical coefficients of *PDE* are consistent with argument that pdf is described by Gaussian and close to the gamma distribution. Thirdly, fluctuations with blobs in the wide SOL are examined in the region (0.4 m ×0.9 m). Figure 7 shows 2D structure of S and k_e in this region. Comparing the flux surfaces it is noticed that these higher order moments are a function of the flux. Both S and k_e are zero or low values for 0.2 m from the LCFS (~ 0.5 m). Outside R > 0.7 m S increases up to 2 and k_e reaches 6 to 7 on the mid-plane. Local maximum of k_e of ~

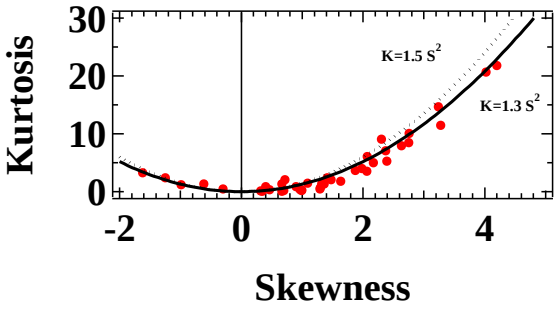

Fig5. Quadratic relation of K and S in the slab plasma.

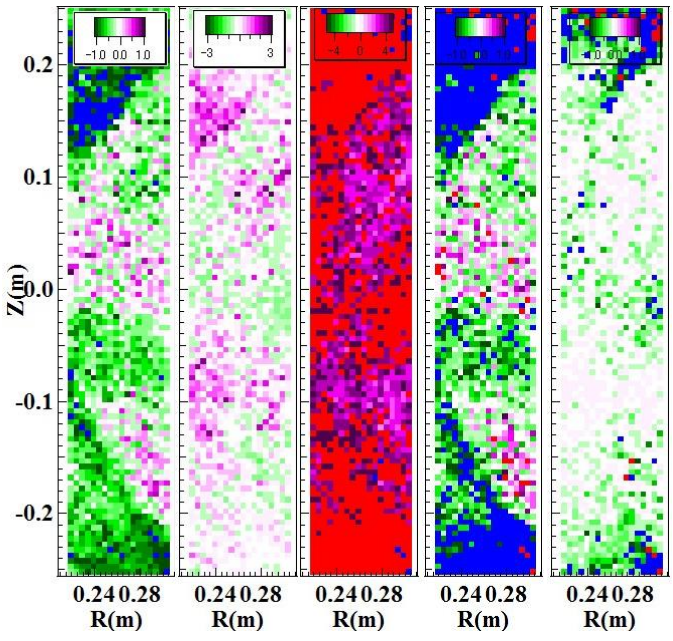

Fig.6 Contours of S, k_e, c_0, c_1 and c_2

10 is found at z~-0.1 m. This zone width of the high S and k_e is 0.15 m. Outside this both are again zero, but this might be ascribed to the reduction of the intensity. This structure also indicates these higher moments are a function of the magnetic field lines. Namely near the top region both values are relatively low and increase towards the mid-plane. Maxima locate below the mid-plane, and they reduce towards bottom. Again simple quadratic relation between S and k_e is found for the entire region.

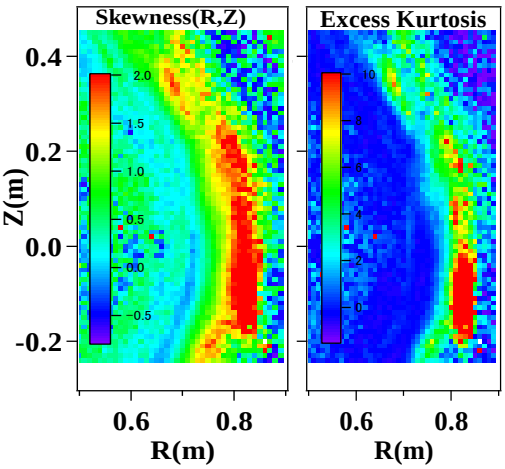

Fig. 7 2D contour of S and k_e

5. Discussion

In QUEST slab plasma, it is observed by analyzing CCD image that the blob is accelerated along the path, where the blob is travelling in R_{sf} region. This acceleration is also confirmed by the E×B flow measurement with scanning probes synchronized with CCD image. Two floating potentials inside the blob are measured when a blob trajectory hits the probes [11]. The blob acceleration near R_{sf} is explained by the 1/R dependence of B_t while E is almost constant form R_{im} to R_{sf}. In DIII-D tokamak, however, it has been observed in [17] that the blob moves radially with $E \times B_t/B^2$ velocities of 2600 m/s near the last closed flux surface LCFS, and ~ 330 m/s near the wall. In TORPEX simple torus geometry it is also observed that the deceleration of the blob from 1750 m/s to 1000 m/s as the blob size is reduced along the path [18]. Numerical simulation of the blob has found that the blob is accelerated when the blob goes down from the density gradient, and it is decelerated when it goes against the density gradient. For non-uniform plasma, blob encounters a force against the density gradient even in the uniform magnetic field [19].

A simple model to describe the density fluctuation X is considered as a stochastic differential equation and a relation between *PDE* and model will be discussed.

$$\frac{dX}{dt} = X(g(X) - s(X)\Lambda(t)) \tag{3}$$

,where g and s are functions of variable X and Λ(t) is standard white noise. When the second term in the r.h.s. is neglect, the fluctuation grows exponentially. The stochastic term regulates the fluctuations and an equilibrium can be assumed. *PDE* can be derived by Ito calculus[20,21],

$$\frac{\partial p}{\partial t} = -\frac{\partial}{\partial X}\left\{\langle M\rangle p - \frac{1}{2}\frac{\partial}{\partial X}(\langle V\rangle p)\right\}, \tag{4}$$

where ⟨M⟩ and ⟨V⟩ are the mean and variance of eq.(3), respectively. If we assume the stationary pdf, the following p(x) is derived.

$$\frac{d(\log P(X))}{dX} = -\frac{\langle V\rangle' - 2\langle M\rangle}{\langle V\rangle} \tag{5}$$

,where $\langle M\rangle = Xg(X)$ and $\langle V\rangle = (\varepsilon X s(X))^2$. $\langle V\rangle'$is a derivative with respect to X and ε is a parameter measuring the amplitude of the random noise. For simple case of s(X) and g(X) eq.(5) belongs to Pearson type eq.2. For the case of density independent noise mode(s(X)=1) and $g(X)=\gamma(1-X/X_e)$ the following gamma distribution can be derived, where at $X=X_e$ a

stationary amplitude of the fluctuation is possible [22],

$$p(X) \propto \frac{1}{\varepsilon^2} X^{\alpha-1} \exp\{-\beta X\}, \qquad \text{if } \alpha>0 \text{ and } \beta>0 \tag{6}$$

where $\alpha=2\gamma/\varepsilon^2$ -1, and $\beta=2\gamma/(X_s\varepsilon^2)=(\alpha+1)/X_s$. As shown in section 4, since the numerical coefficients can be derived from higher order moments, these parameters ($\alpha\beta$) can be deduced implicitly. From this procedure validation of the model equations is possible.

6. Conclusion

Statistical features of fluctuations are investigated using the CCD imaging technique in open and closed magnetic configurations. Intermittency dominated by blobs is observed in open configuration in slab and outer SOL plasmas. From the statistical point of view there is no significant difference between fluctuations in both configurations. Inside the LCFS the pdf can be described well by Gaussian one and the deviation form it is small. In the open field region it is observed that a simple quadratic relation exists between S and k_e and the deviation of the pdf from Gaussian is considered to be caused only by the field line properties. This conclusion is supported the fact of two dimensional structure of the higher order moments as a function of the magnetic surfaces. These moments become also a function of the filed lines.

Acknowledgements

This work is supported by a Grant-in-aid for Scientific Research (A21246139). This work is also performed with the support and under the auspices of the NIFS Collaboration Research Program (NIFS07KOAR009, NIFS08KUTR024).

References

[1] S. J. Zweben, et al., Phys. Fluids **28** 974 (1985)
[2] S.J. Zweben, et al., Nucl. Fusion **44** 134-153 (2004).
[3] S.J. Zweben, et al., Phys. Plasma **9** 1981 (2002)
[4] G.Y. Antar, et al., Phys. Rev. Lett. **87** 065001 (2001)
[5] D.A.D'Ippolito, Contrib. Plasma Phys. **44** 205-216 (2004).
[6] I. Furno, et al., Phys. Plasma **15** 055903 (2008).
[7] O.E. Garcia et al., Phys. Rev. Lett. **92** (2004).
[8] S.I. Krasheninnikov and A.I. Smolyakov Phys. Plasma **14** 102503 (2007)
[9] H. Zushi, N. Nishino et al., accepted for publication in J. Nucl. Mater (2010).
[10] F.M. Poli, et al., Phys. Plasma **15** 032104 (2008)
[11] Q.H. Lui, et al., J. Plasma and Fusion Research series **9** 33-36 (2010)
[12] F. Sattin, et al., Plasma Phys. Contr. Fusion **51** 055013 (2009)
[13] B. Labit et al., Phys. Rev. Lett. **98** 255002 (2007).
[14] N. L. Johnson, S. Kotz, N. Balakrishnan, "Continuous univariate distribution" Vol.1 and 2 2nd edition Wiley Series in probability and mathematical statistics
[15] T. Kikukawa H. Zushi et al., J. Plasma and Fusion Research **3** 010 (2008)
[16] R. Bhattacharyay, H. Zushi et al., Phys. Plasma **15**, 022504 (2008)
[17] J.A. Boedo, et al., Phys. Plasma **10** 1670 (2003)
[18] S. H. Müller, et al., Phys. Plasma **14** 110704 (2007)
[19] K.Bodi et al., J. Nuclear Mater. **390-391** 359-363 (2009)
[20] R.F.Costantino and R.A. Desharnais J. Animal Ecology **50** 667-681 (1981)
[21] M. Turell, Theoretical population biology **12** 140-178 (1977)
[22] B. Dennis, G.P. Patil, Math. Bioscience **68** 187-212 (1984)